Publ. Astron. Soc. Japan 39, 573–587 (1987)

Thermal and Nonthermal Emission Structures in the Galactic Center Region

Wolfgang REICH,[1,2] Yoshiaki SOFUE,[2,3] and Ernst FÜRST[1]

[1]*Max-Planck-Institut für Radioastronomie, Auf dem Hügel 69, 5300 Bonn 1, F.R.G.*
[2]*Nobeyama Radio Observatory,* Minamimaki-mura, Minamisaku-gun, Nagano 384-13*
[3]*Department of Astronomy, Faculty of Science, University of Tokyo, Bunkyo-ku, Tokyo 113*

(Received 1987 May 11; accepted 1987 July 29; revised in proof 1987 August 31)

Abstract

By a detailed comparison of background-filtered maps of the 11-cm (2.695-GHz) radio continuum emission and the 60-μm infrared emission for the central $2^\circ \times 3^\circ$ region of the Galaxy we were able to separate nonthermal and thermal emission structures. Based on this comparison we found that the "galactic center lobe (GCL)" basically has nonthermal characteristics. Near Sgr A two possibly nonthermal spurlike structures are noted. The nuclear disk shows unusual high infrared emission. A previously unrecognized supernova remnant was identified.

Key words: Galactic center; Infrared emission; Radio continuum emission; Supernova remnants.

1. Introduction

The flat radio spectra and recombination lines observed towards the central few degrees of the Galaxy had led us to consider that the radio emission is thermal due to ionized hydrogen (H II) gas (Mezger and Pauls 1979). However, recent high-resolution radio observations (Yusef-Zadeh et al. 1984) and polarization measurements (Seiradakis et al. 1985; Tsuboi et al. 1986; Sofue et al. 1987) of the galactic center region revealed that a considerable fraction of the emission is nonthermal (synchrotron) and the existence of a strong magnetic field has been established. Therefore, the flat or rather inverted spectra which are observed for most of the features in the central region (Sofue 1985; Reich et al. 1987) are not necessarily an indicator of thermal emission. The peculiar morphological structures of scales from ~ 1 pc to ~ 100 pc are believed to be linked to the central activity (e.g., Lo 1986), but their physical characteristics and origin are far from being clarified. In order to understand

* Nobeyama Radio Observatory, a branch of the Tokyo Astronomical Observatory, University of Tokyo, is a facility open for general use by researchers in the field of astronomy, astrophysics, and astrochemistry.

the origin and physical characteristics of the features, we need at least to know whether the emission is of thermal or nonthermal nature.

Recently we (Fürst et al. 1987) have analyzed the correlation between the galactic radio continuum emission at 11 cm observed by Reich et al. (1984) and the far-infrared (FIR) emission observed by IRAS (Beichman et al. 1985). Among the four wavelengths of the IRAS survey we have found a particularly good linear correlation between the radio and the 60-μm intensities for optically thin thermal sources (H II regions), where the FIR emission originates from coexisting dust grains heated by thermal electrons (e.g., Fazio 1978). On the contrary, nonthermal (synchrotron) radio features like supernova remnants are hardly seen in the IRAS maps, firstly because the synchrotron emission has a steep spectrum at wavelengths shorter than millimeters, even though it has a flat spectrum in the radio domain. Secondly, even in old supernova remnants the FIR emission of shock heated dust is weak compared with the FIR emission of H II regions. This fact led us to conclude that nonthermal emission objects, even though their radio spectra are flat, can easily be distinguished from thermal sources by comparing the IRAS and radio maps.

More quantitatively, the observed ratio of surface brightness at 60 μm to that at 11 cm, $R=\Sigma_{60\ \mu\mathrm{m}}/\Sigma_{11\ \mathrm{cm}}$, for H II regions is larger than 300 with the majority concentrating around $R=1000$, whereas the ratio is less than ~ 300 for nonthermal sources like supernova remnants (Fürst et al. 1987). In case of H II regions the ratio R is an equivalent quantity to the "infrared excess (IRE)" introduced by Emerson and Jennings (1978), which they define as the ratio of the infrared luminosity integrated between 40 and 350 μm to ionizing-photon number that is proportional to free-free radio intensity.

In this paper we try to distinguish the thermal and nonthermal features in the galactic central $2^\circ \times 3^\circ$ region based on the idea of Fürst et al. (1987).

2. Data Analysis

We made use of the data from the 11-cm (2.695-GHz) survey of the galactic plane by Reich et al. (1984) and of the 60-μm data observed by IRAS (Beichman et al. 1985; see also Gautier et al. 1984). We selected a field of $2\overset{\circ}{.}2 \times 3^\circ$ centered on $l, b=0^\circ, 0^\circ$ (=figure 4 of Reich et al. 1984). The data were scaled in mJy/beam of the 11-cm survey beam (HPBW=$4\overset{'}{.}27$) following Fürst et al. (1987) and the relative zero level was defined at galactic latitude $\pm 1\overset{\circ}{.}5$. We subtracted the smooth diffuse "background" emission by applying the "background filtering (BGF)" technique described by Sofue and Reich (1979). We used a filter beam of $0\overset{\circ}{.}3 \times 0\overset{\circ}{.}3$ and ran 12 iterations, which was found to give the best separation between individual structures and a smooth "background" for this complex emission region with very steep intensity gradients. The smooth background emission consists of several components: diffuse galactic emission, broadly distributed, small-scale components which merge to a smooth distribution at the resolution used, and zodiacal emission, which is still important at 60 μm. The zodiacal emission is assumed to vary only gradually across the area investigated in this paper.

The results of the decomposition of the 11-cm and the 60-μm maps are shown

in figures 1 and 2, respectively, after convolving the data to a common angular resolution of 6′. As done by Fürst et al. (1987), we calculated a difference map between the radio and infrared source emission shown in figure 3. Here the "difference" is defined as $\Delta\Sigma=\Sigma_{11\,\mathrm{cm}}-\Sigma_{60\,\mu\mathrm{m}}/1000$ (Jy/beam). $\Delta\Sigma$ is positive for nonthermal sources and around zero or negative for high infrared excess sources like H II regions. However, differences are dependent on the absolute source strength and therefore we calculated the ratio $R=\Sigma_{60\,\mu\mathrm{m}}/\Sigma_{11\,\mathrm{cm}}$ for regions where the 11-cm intensity exceeds 100 mJy/beam. The result is shown in figure 4.

3. Results

a. General Distribution of the FIR-to-Radio Ratio, R

In regions in figure 4 with $R<300$ a dominant contribution from nonthermal emission is indicated. Normal H II regions have values of $R\sim1000$ with some scatter, while high infrared emission regions with weak thermal free-free emission have values $R\geq2000$. Because of line-of-sight effects it is obvious that in many regions some mixture of different emission features superpose.

Figure 5 shows histograms of the frequency distribution of R for the galactic center region (figure 4) and for comparison the distribution found for a "normal" galactic plane region, i.e., the region between $l=25°$ and $l=31°$ studied by Fürst et al. (1987), normalized for the same number of data points. As seen from figure 5 in the latter region the majoritiy of sources are normal H II regions resulting in a sharp peak at $R=1000$, and a small portion of sources are nonthermal with $R=0$ identified with supernova remnants and a few extragalactic sources. Compared to this region, there are obviously more sources near the galactic center area showing characteristics of nonthermal emission. This fact seems to be related to energetic phenomena occurring in the central region. Also we note that the fraction of the extremely "dusty" tail with large values of R exceeds that in normal interstellar space significantly. This may indicate that in the galactic center region a large number of dust clouds are located which are not evolved to high-mass star formation sites (H II regions) so that less free-free emission is radiated (see subsection 3f), whereas in normal H II regions dust and gas are well related within the present beamwidth of 6′.

Below we describe some prominent features noticed from comparison of the radio and infrared maps. We are particularly interested in a separation of nonthermal and thermal features among the various emission structures.

b. The Galactic Center Lobe

In the radio map (figure 1a) two hornlike ridges are seen, emerging vertically from the galactic plane at $l=359\overset{\circ}{.}4$ and at $l=0\overset{\circ}{.}2$ towards positive latitudes. These structures are hardly seen in the IRAS map (figure 2a) except for a broad weak FIR emission feature along the western ridge. These vertical ridges are part of the "galactic center lobe (GCL)" and are probably caused by a large-scale ejection (jet) phenomenon occurring in the galactic center (Sofue and Handa 1984; Sofue 1985).

The eastern radio ridge is linked to the radio arc crossing the galactic plane at $l=0\overset{\circ}{.}2$, and further extends towards negative latitudes down to $b\approx-1°$. Although

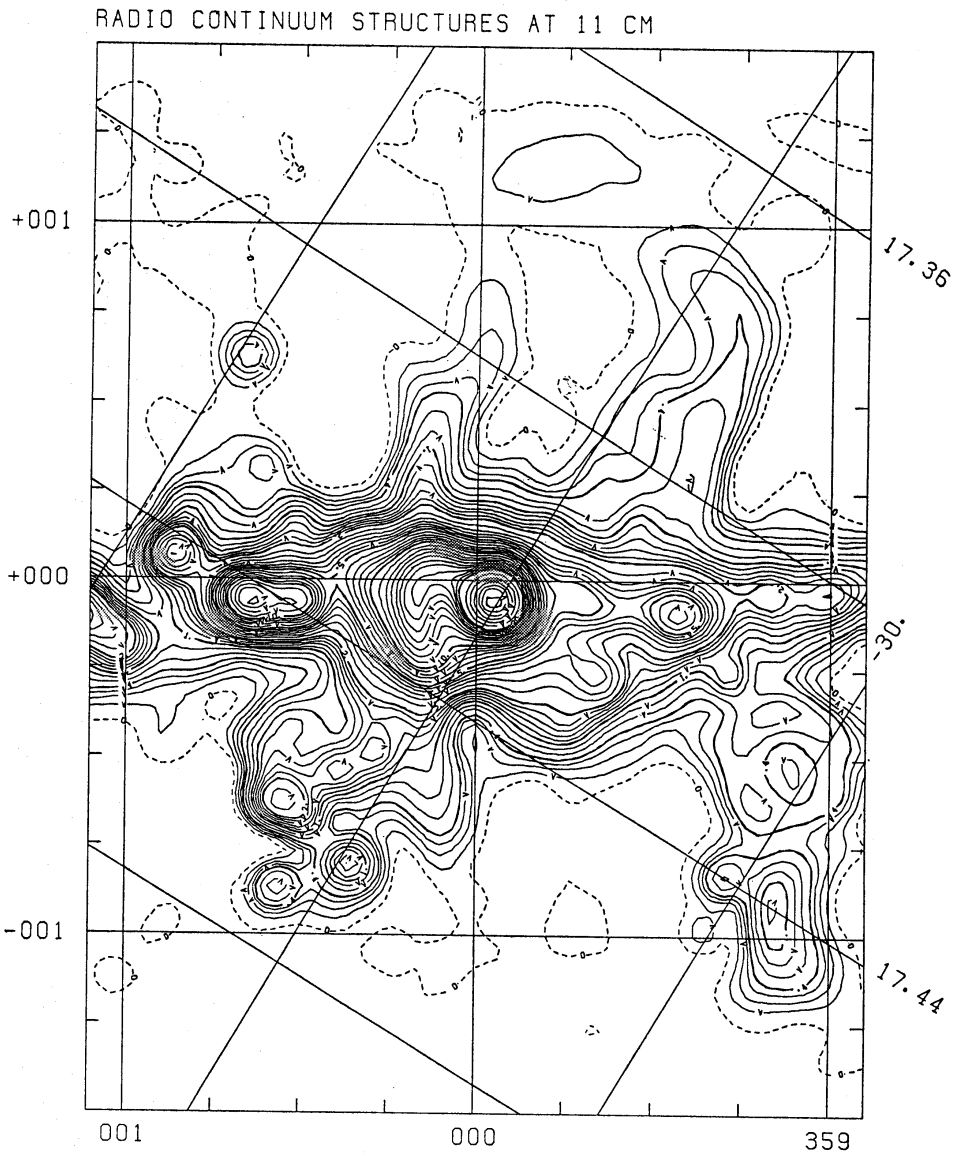

Fig. 1a. 11-cm radio continuum emission of the central region of the Galaxy reproduced from Reich et al. (1984) after subtraction of the smooth "background" emission as shown in figure 1b and smoothed to 6′. Coordinates are in l, b with a superposed grid of equatorial coordinates for epoch 1950. Contours are labeled in Jy/beam. Contour lines are shown at 0, 0.1, ···0.4, 0.6, ···2, 2.5, ···5, 6, ···10, 12, ···30, 40, ···90 Jy/beam. The arrows (∨) on the contour lines point towards the minimum direction.

the whole GCL has a flat radio spectrum (Sofue 1985), the eastern ridge is highly polarized at 3 cm and 6 cm (Seiradakis et al. 1985; Tsuboi et al. 1986; Sofue et al. 1987) and is certainly a nonthermal object associated with a strong magnetic field of a few tens of micro-Gauss.

The nature of the western part of the GCL is similar to that of the eastern part and to the SNRs at G359.1−0.5 and G359.1−0.9, which follows from the fact that the average ratio R is around 300. This indicates that the emission in the western part is also nonthermal. At l=359°.5, b=0°.4 a small dust cloud is located, which

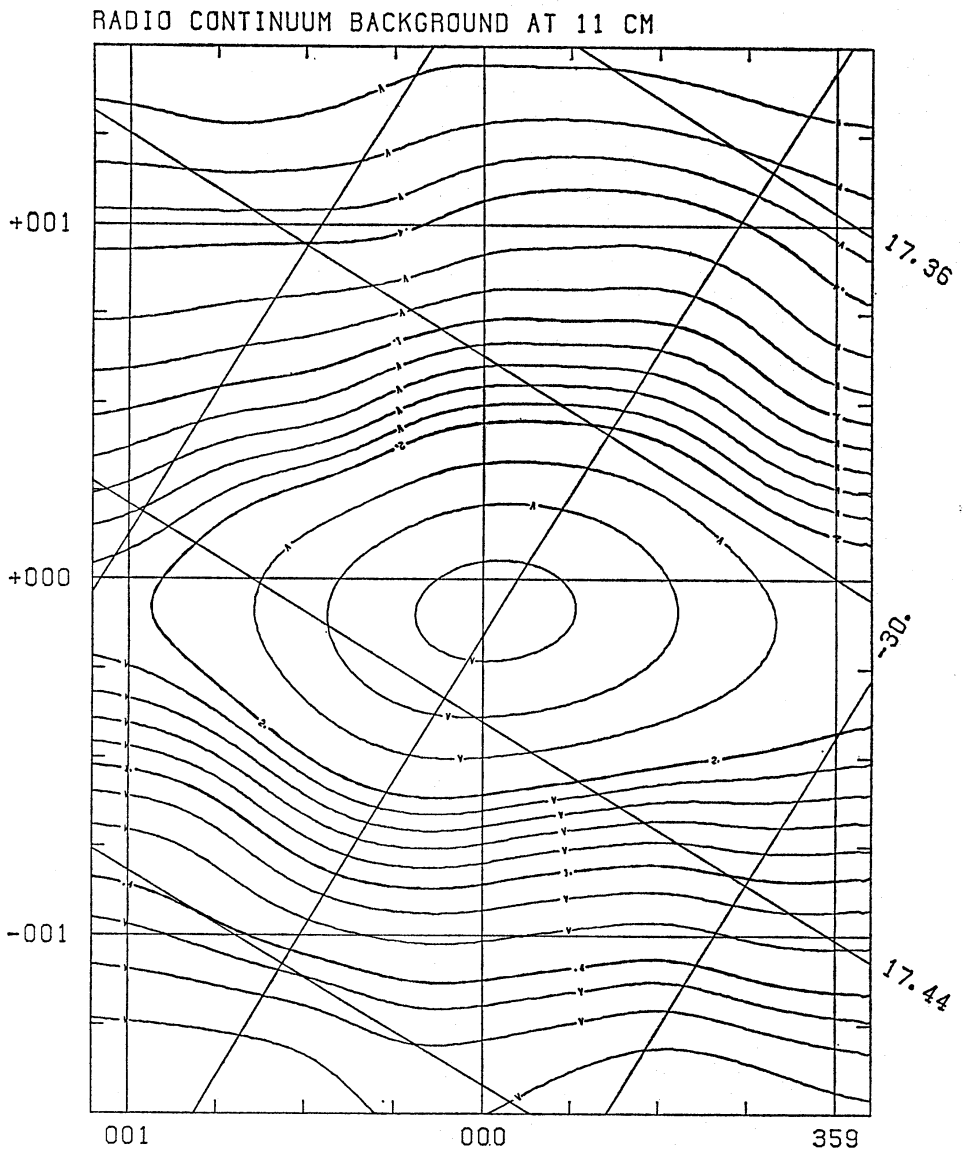

Fig. 1b. The smooth "background" component at 11-cm wavelength. Contour steps are the same as in figure 1a.

is most prominent at 25 μm and causes some increase of R in this area. This cloud seems to be unrelated to the GCL. The value of R decreases to values around 0 in between the eastern and western ridges of the GCL, so that the emission of this area seems to be completely nonthermal. At the outer gradient of the western ridge R increases to values above 600 indicating the presence of some thermal emission. In fact, figures 2a and 2b indicate that weak FIR emission surrounds the western part of the GCL.

No radio polarization was detected at the western ridge (Tsuboi et al. 1986) and its emission mechanism was not clarified from the radio observations alone. The lack of detectable polarization may be attributed to depolarization by the thermal gas surrounding the western part of the GCL. The eastern ridge is not associated

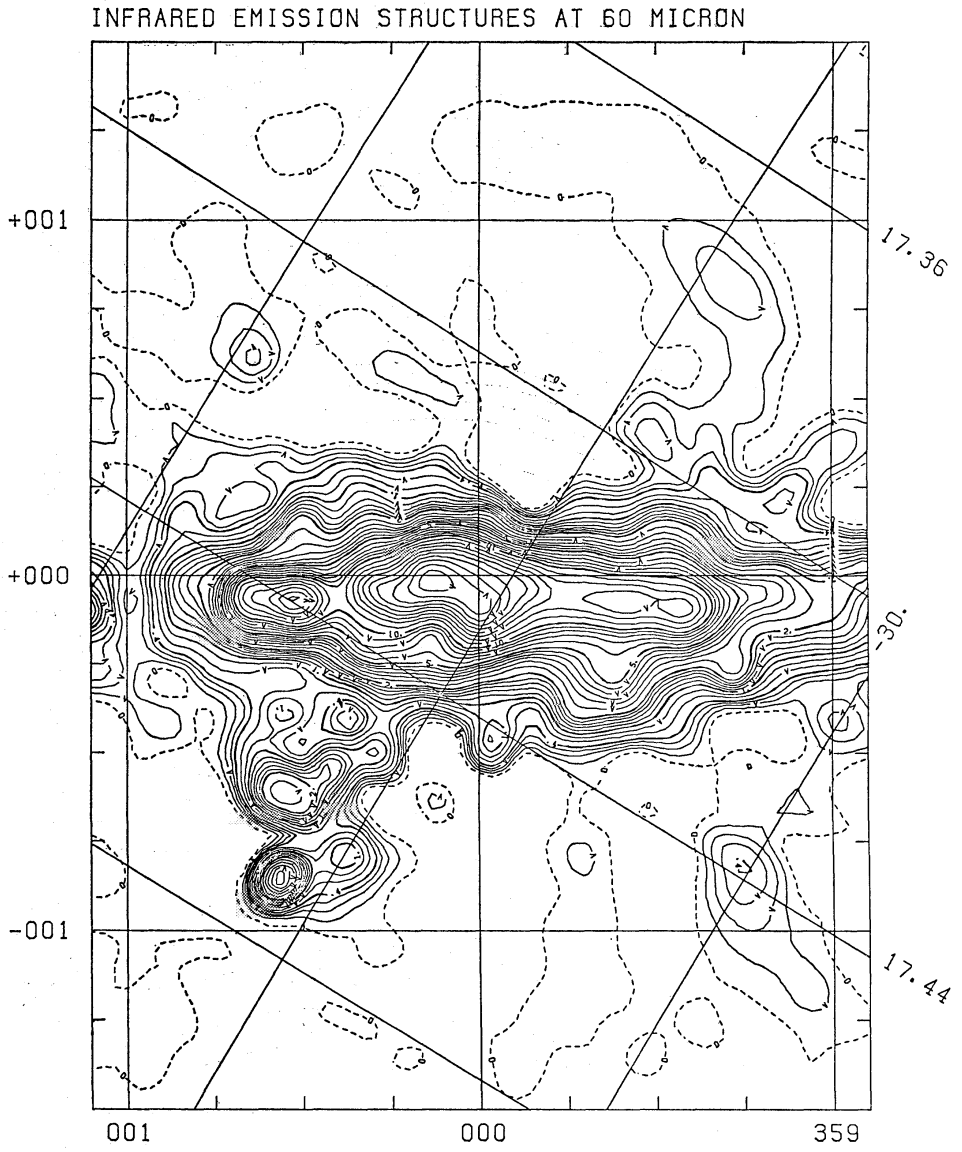

Fig. 2a. 60-μm infrared emission of the central region of the Galaxy taken from the IRAS data (Beichmann et al. 1985) at 6′ angular resolution after subtraction of the smooth "background" emission as shown in figure 2b. Contours are labeled in 1000 Jy/beam. Contour steps are the same as in figure 1a, but multiplied by 1000.

with thermal gas so that no depolarization occurs. If the total radio emission of the western arc is nonthermal, the magnetic field strength can be derived from the assumption of equipartition. We get a few 10^{-5} G, about the same value, which was derived for the eastern ridge. If the magnetic field along the western ridge runs parallel to it, as it is the case for the eastern ridge, the magnetic field penetrates the galactic plane at l=359°.4, where Sgr C is located. The vertical direction of the magnetic field is supported by the detection of a radio filament in Sgr C perpendicular to the galactic plane (Liszt 1985).

According to Sofue and Fujimoto's (1987) model, the eastern and western ridges of the GCL are parts of a large-scale vertical magnetic field in the central region of

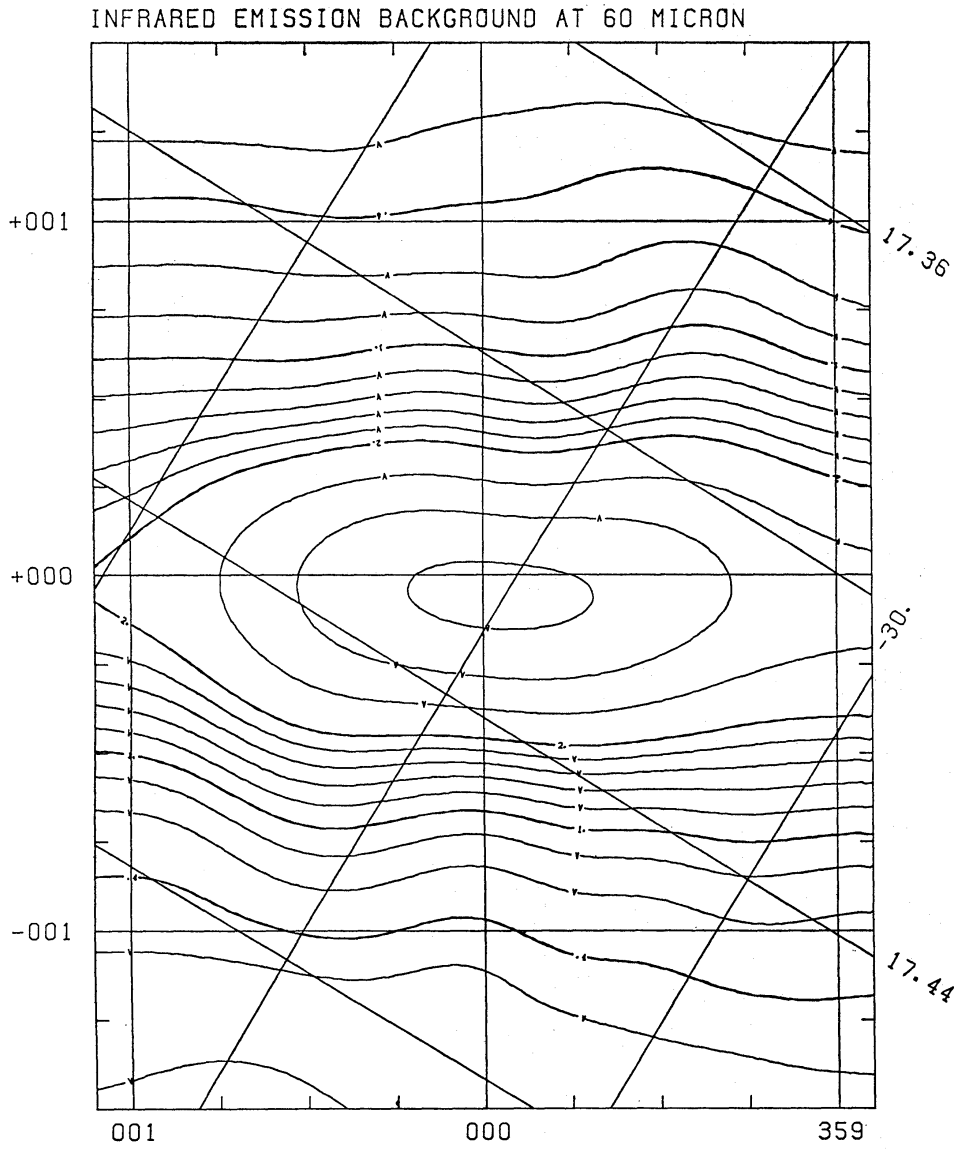

Fig. 2b. The smooth "background" component at 60 μm. Contour steps are the same as in figure 2a.

the Galaxy, which are illuminated by jets emerging from the galactic center. The eastern ridge is an extension of the radio arc being just hit by the jet. The shocked jet is observed as the complicated radio bridge between the arc and Sgr A. The strong polarized emission along the eastern ridge is caused by synchrotron radiation of electrons which are accelerated through the interaction of the magnetic jet and the vertical field. The associated injection of thermal gas by the jet from the "bridge" area (the region between Sgr A and the vertical arc structure) causes a strong Faraday rotation resulting in a sharp depolarization of the emission near the intersection of the jet and the arc. The thermal gas has not yet spread to the upper parts of the ridge so that in the higher-latitude regions of the eastern ridge the radio emission is not depolarized.

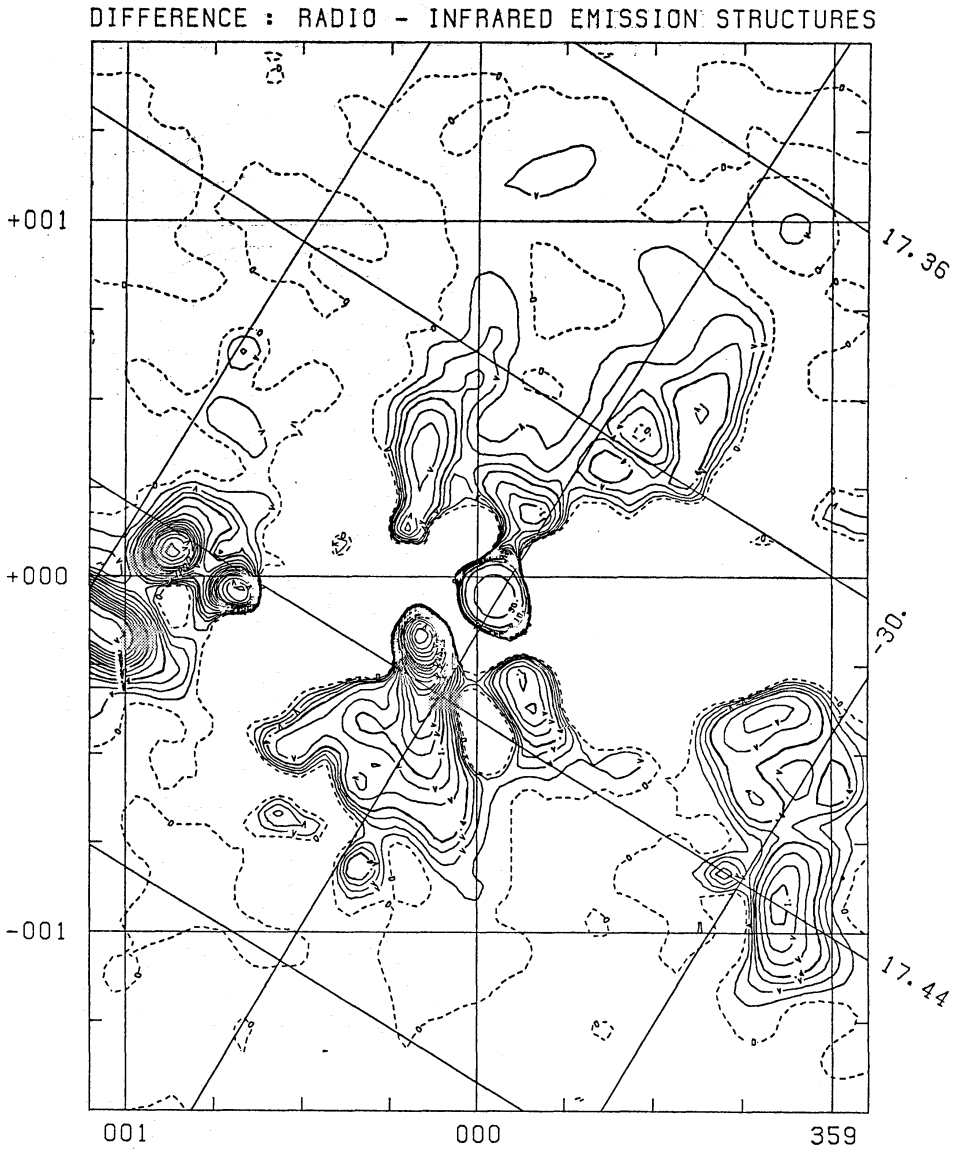

Fig. 3a. Difference of the radio emission (figure 1a) and the infrared emission (figure 2a, divided by 1000): $\Delta\Sigma=\Sigma_{11\,\mathrm{cm}}-\Sigma_{60\,\mu\mathrm{m}}/1000$. Contours are shown as for figure 1a.

Contrary to that the western ridge is probably an older synchrotron tube which was illuminated in the past by another jet. The Sgr C filament (Liszt 1985) is a remnant of a jet-illuminated magnetic field from that time located at the root of the western ridge. The thermal gas ejected by this older jet has already widely spread over the western ridge along the magnetic field lines. This results in a large internal Faraday rotation and causes the depolarization along the whole western ridge. This may well explain the asymmetric polarization properties between the eastern and western ridges (Tsuboi et al. 1986).

The association of thermal gas and dust at the outer edge of the western ridge is also consistent with the "mild-jet" model of the GCL-formation as proposed by Uchida et al. (1985). Morphologically the surrounding thermal gas composes a

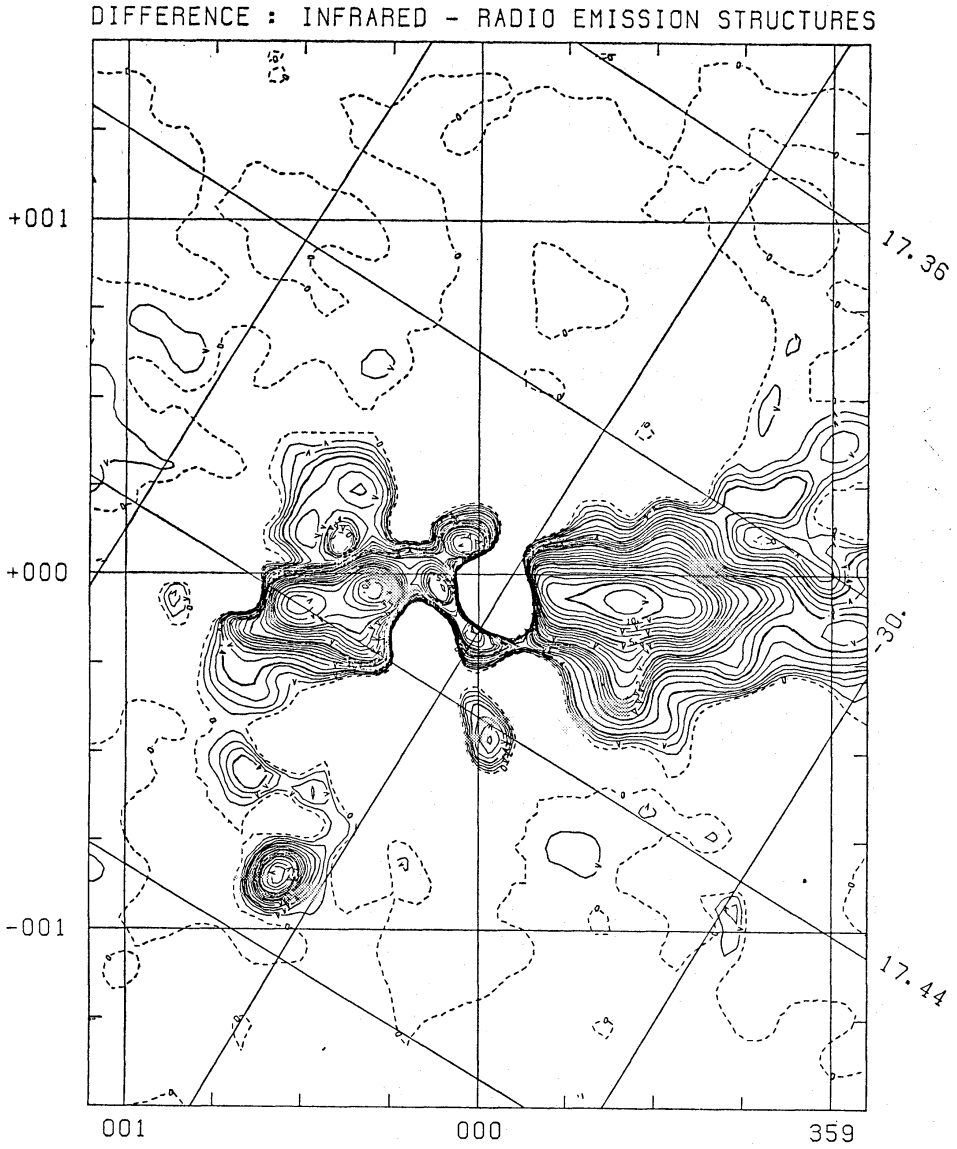

Fig. 3b. Difference of the infrared emission (figure 2a, divided by 1000) and the radio emission (figure 1a): $\Delta\Sigma=\Delta\Sigma_{60\ \mu m}/1000-\Sigma_{11\ cm}$. Contours are shown as for figure 1a.

shell around the western part of the GCL. This distribution may alternatively be explained in terms of gas, which was shock-compressed by an explosion which occurred in the galactic center some 10^6 yr ago (Sofue 1984).

c. Other Nonthermal Structures Possibly Connected to the Galactic Center

Besides the GCL and some supernova remnants (subsection 3d) we note other apparently nonthermal structures. One remarkable feature is located at $l=359\overset{\circ}{.}8$, $b=-0\overset{\circ}{.}3$ to $b=-0\overset{\circ}{.}5$ (figures 3a and 4). This feature extends along the direction of the steep spectrum low-energy jet emanating from Sgr A (Yusef-Zadeh et al. 1986; Kassim et al. 1986), which can be traced down to $b=-0\overset{\circ}{.}3$. At 11-cm wavelength (figure 3a) we note a gap at $b=-0\overset{\circ}{.}3$. It is not clear whether this gap is real or due

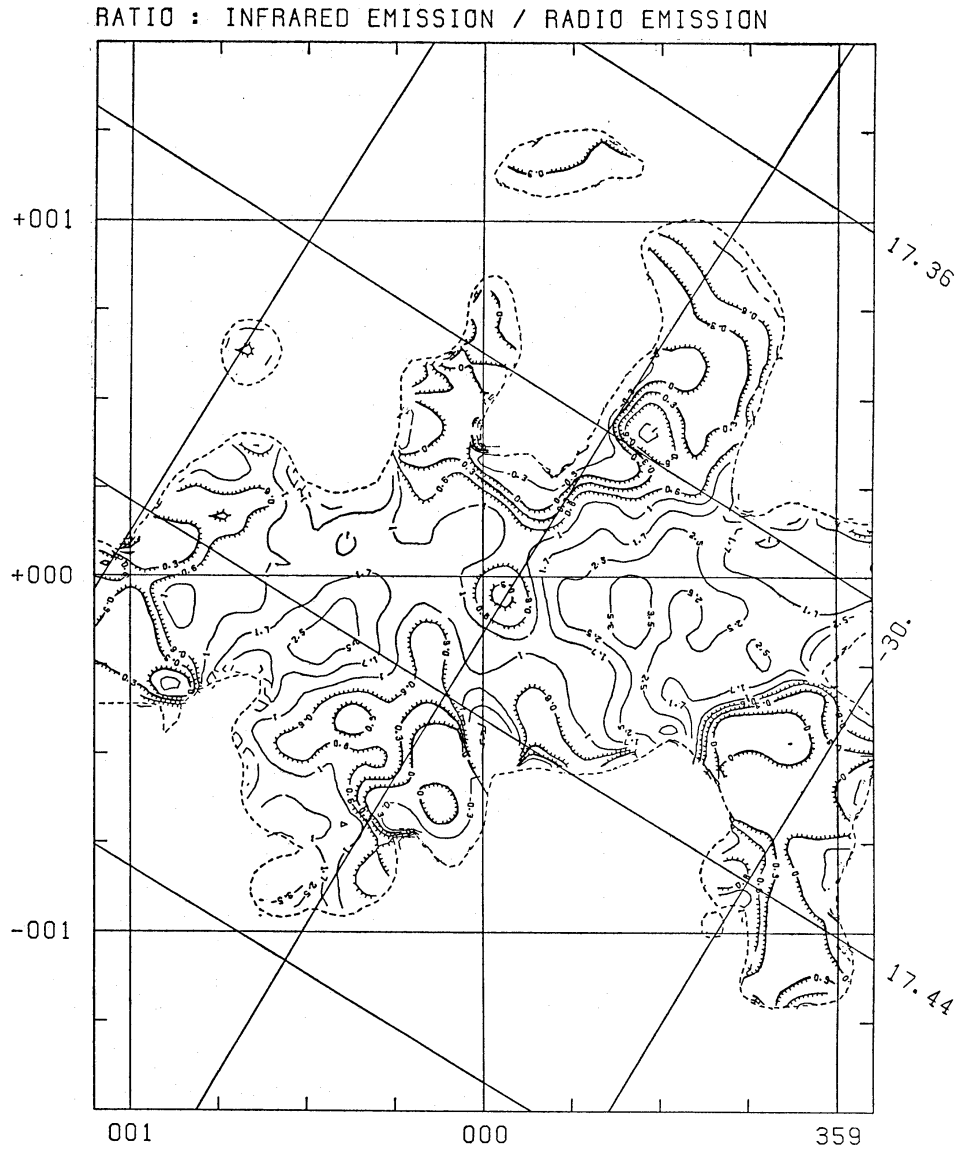

Fig. 4. Map of the ratio $R=\Sigma_{60\,\mu m}/\Sigma_{11\,cm}$ (e.g., figures 2a and 1a) for regions with 11-cm intensities exceeding 100 mJy/beam (shown by the dashed contour line). Contour labels show values of R divided by 1000. Contours with ticks are for $R<600$, where nonthermal emission dominates, while regions with thin contours ($R>600$) are mostly thermal emission regions.

to limitations in the applied BGF method at the extremely steep gradient of Sgr A. The 11-cm emission at $b<-0^{\circ}3$ may be explained as nonthermal emission of an extension of the low-frequency jet towards lower galactic latitude. In this case the missing low-frequency emission of this extension at frequencies up to 843 MHz (Yusef-Zadeh et al. 1986) requires very high thermal absorption. Alternatively, if the presently detectable jet is the relic of a much more energetic event in the past, this event might have blown a large cavity or channel into the interstellar medium so that the missing dust causes the apparent value of R near zero. In this case the derived nonthermal emission is just an artifact.

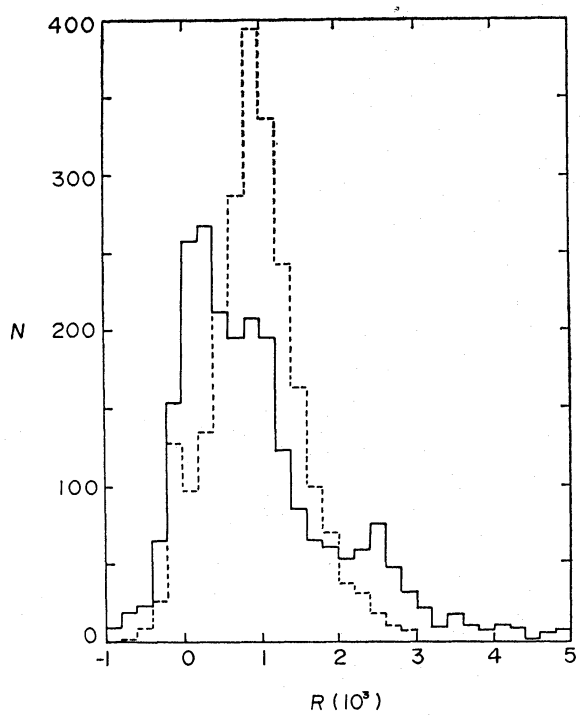

Fig. 5. Histograms of the frequency distribution of R for the galactic center region (full line) and for the region $l=25°$ to $l=31°$ (dashed line; Fürst et al. 1987) normalized for the same total number of data points.

Another feature that seems to be related to Sgr A is located at $l=359°.8$, $b=0°.1$ to $b=0°.3$ with its upper part being merged with the inner nonthermal region of the GCL. This apparently nonthermal feature is located along the NE-direction of "threads" and "parabolic protrusions" emerging from Sgr A West as observed by Morris and Yusef-Zadeh (1985) and Yusef-Zadeh (1986).

d. Supernova Remnants

Three known supernova remnants (SNR's) are located in the galactic center region. G359.1−0.55 is a shell-type SNR with a diameter of 24′ and a spectral index of $\alpha=-0.37$ ($S\sim\nu^{\alpha}$) in the wavelength range between 11 cm and 6 cm (Reich and Fürst 1984). Its distance is unknown. An application of various published Σ–D relations results in distances between 4 kpc and 13 kpc or diameters between 30 pc and 90 pc (Reich and Fürst 1984).

G0.9+0.1 is a combined-type SNR, as it was recently shown by Helfand and Becker (1987). It consists of a 8′ shell with a spectral index of $\alpha=-0.6$ and a 2′ flat spectrum core with $\alpha=-0.1$. Its distance is unknown.

G1.05−0.1 was identified by Downes et al. (1979) as an SNR with a diameter of 6′ and a spectral index of $\alpha\approx-0.65$. The distance of G1.05−0.1 is unknown.

All three objects clearly show up at 11-cm wavelength, but are very weak at 60 μm (e.g., figure 3a). The ratio R for these sources is between 0 and 300 (figure 4) confirming their nonthermal nature and their identification as SNR's.

Another source with a nonthermal characteristic is G359.0−0.95, an incomplete

half shell of 23′ diameter. Its flux density is 14±2 Jy at 11-cm wavelength. We have measured 12.2±2 Jy at 6-cm wavelength (4.75 GHz) with the Effelsberg 100-m telescope. From the radio survey at 3-cm wavelength (10.3 GHz) of Handa et al. (1987) a flux density of 6.8±2 Jy is obtained. The radio spectral index is $\alpha=-0.5\pm 0.3$. At 6-cm wavelength the integrated polarization percentage of G359.0−0.95 is 3.5%.

No distances are available for all these SNR's. We like to mention that the number density of SNR's in the galactic center region (8 SNR's/5° longitude range) is about twice the average value (~4 SNR's/5°) for the area $|l|\leq 20°$, $|b|\leq 1°.0$, based on the recent SNR catalog of D. A. Green (1987, private communication). This indicates that some SNR's may be physically located near the galactic center.

e. Sgr A, B, and C

The strongest radio sources in the galactic center region, namely Sgr A, B, and C, are located close to $b=0°$, within the nuclear disk of ionized thermal gas with radius and thickness of $\sim 0°.8\times 0°.3$ [120 pc × 40 pc at 8.5-kpc distance; Mezger and Pauls (1979)].

Sgr A appears as a nonthermal source (see figures 3a and 4). However, based on its integrated radio spectrum for an area of 15′ in diameter as measured by Reich et al. (1987), the nonthermal component at 11-cm wavelength is of the order of 20% of the total intensity. Comparing the radio map (figure 1a) and the IRAS 60-μm map (figure 2a) different morphologies are seen in the area of Sgr A. The infrared structures seen at 12 μm and 25 μm resemble the radio structures much more. Different dust components are superposed in the Sgr A area and, therefore, the comparison between the 11-cm emission and 60-μm emission is insufficient to disentangle the thermal and nonthermal components of Sgr A.

Sgr B (G0.67−0.03) is known to be a compact H II region, while it appears as a strong radio-excess source in figure 3a. This results from its IR-to-radio ratio, R, which is slightly below 1000 (see figure 4) and from its absolute strength. The same tendency was already recognized for the compact H II region W43 (G30.8−0.05; Fürst et al. 1987). The fact that the radio emission compared with the IR-emission has an excess over that in normal H II regions may indicate that intense star forming regions are associated with some nonthermal radio emission or that dust grains in these regions are more dissociated compared to normal H II regions due to the intense UV-light from very young stars.

While Sgr A and B are strong enough and therefore not much affected from its surroundings, Sgr C (G359.4−0.07) is severely confused with its surrounding high IR-excess emission, so that it is not possible to discuss its proper IR/radio characteristics from the present data. Higher-resolution observations are necessary to separate the source from the background.

f. The Nuclear Disk

The extended infrared emission is much more intense than expected from the radio emission, even if it is completely thermal (see figures 3b and 4). We discussed this already in subsection 3a. The comparison of the background emission in figures

1b and 2b shows that the IR-to-radio ratio R ranges between 800 and 1200, indicating a thermal characteristic in general. The resemblance of the general IR and radio distributions has been pointed out by Maihara et al. (1979) from their $0^{\circ}.7 \times 1^{\circ}$-resolution observations at 150 μm. These facts confirm the existence of the nuclear disk of ionized thermal gas as found by Mezger and Pauls (1979).

However, a more detailed comparison reveals that the radio emission in figure 1b has a broader distribution around the galactic center compared with the IR-background (figure 2b) which flattens towards the galactic plane. This trend is seen in figure 2a as well and indicates that the region close to the galactic plane is rich in dust not well mixed with ionized gas. In fact the high-IR excess tail of the R-frequency histogram (figure 5) is mostly due to this ridge of IR emission near the galactic plane. We point out that the galactic center region contains a wealth of clumpy molecular clouds (e.g., Bally et al. 1987), which are not necessarily associated with individual H II regions. We may conclude that, although the star forming activity in total is much higher near the galactic center than in normal disk regions of the Galaxy, the relative amount of molecular clouds that have not been dissociated and/or ionized is higher in the center region as well, while the dust is enough heated to radiate strong IR emission.

This could be explained by a different mass function of stars in the nuclear disk; low-mass stars dominate and radiate enough light to heat the dust, while high-mass stars, which radiate UV-photons to dissociate the dust and ionize the hydrogen, are less abundant compared to the normal interstellar space. Alternatively, if the mass function were the same as in the normal disk region, the high IR-excess and therefore heating of the molecular gas must be done in another way. It may be caused by the galactic center activity and/or thermalization of kinetic energy of the disk rotation. As the heating is observed throughout the disk, the center activity may not be the reason. In the other case, the IR luminosity of $\sim 10^{41}$ erg s^{-1} would require dissipation of the rotation energy of the nuclear gas disk in $\sim 10^{7}$ yr or in several rotations and cause a very rapid contraction of the gas towards the center. This seems also unlikely.

g. H II Regions

Most of the discrete compact and extended sources, which are seen both in the radio and IRAS maps, are regarded as H II regions from their flat radio spectra and recombination-line detections. There exists a complex of local H II regions around G0.6−0.6 (Downes et al. 1979), which is composed of several bright knots distributed over an area of 30′ in diameter. These sources are clearly seen both in the radio and infrared maps (figures 1a and 2a). One of them, G0.55−0.85, is identified with the H II region RCW 142 embedded in a dense molecular cloud, no more distant than the Sagittarius arm (Gardner and Whiteoak 1975). This source is exceptionally strong at 60 μm, as seen in figures 3b and 4. To the western and northern side of this complex, close to the southern extension of the arc region, there is an indication of a nonthermal emission component (figures 3a and 4).

h. Infrared Objects without Radio Counterparts

Figure 2a shows a strong, compact infrared source, G359.9−0.45, located in a

region of minimum radio emission (figure 1a). The nature of this object is unknown.

Another more extended structure with no corresponding radio emission is located at $l, b = 359\overset{\circ}{.}3, -0\overset{\circ}{.}9$. It is more pronounced at 100 μm than at 60 μm. This indicates a low dust temperature, more typical for molecular clouds than for H II regions. The small-diameter radio source G359.3−0.83 is located in the direction of that dust cloud. It has a flat spectrum up to 3-cm wavelength ($\alpha = -0.19$; Handa 1987). At 6-cm wavelength we observed 1.3 Jy and 9.7% of linear polarization with the Effelsberg 100-m telescope (HPBW $2\overset{'}{.}4$). The source appears slightly extended ($\approx 1'$ diameter). The nature of this object is unclear; however, it is likely unrelated to the extended infrared emission.

4. Concluding Remarks

We have shown that the combination of the 11-cm survey map and the 60-μm IRAS map of the galactic center region provides a powerful tool to distinguish between nonthermal and thermal sources, even if the former have flat radio spectra. The present method has a great advantage to the previous method to identify nonthermal emission by polarization observations particularly for distant galactic plane regions, where high depolarization is often observed. We also emphasize that diffuse thermal emission regions, where recombination-line observations are rather difficult, can be easily distinguished from nonthermal emission regions using the present method. This was shown to be particularly effective for such a region as the GCL, which is basically a nonthermal structure. A new SNR could be identified. A limitation of this global method was found for the areas near Sgr A and Sgr C.

This work was done as part of an international research exchange program between NRO and MPIfR under the financial support of the Japan Society for the Promotion of Sciences and of the Max-Planck Gesellschaft. One of the authors (Y.S.) thanks the Japanese Ministry of Education, Science, and Culture for the financial aid under Grant No. 61460009. We thank Dr. Patricia Reich for software support.

References

Bally, J., Stark, A. A., Wilson, R. W., and Henkel, C. 1987, *Astrophys. J. Suppl.*, in press.

Beichman, C. A., Neugebauer, G., Habing, H. J., Clegg, P. E., and Chester, T. J. (ed.) 1985, *IRAS Explanatory Supplement 1985*, JPL D-1855 (Jet Propulsion Laboratory, Pasadena).

Downes, D., Goss, W. M., Schwarz, U. J., and Wouterloot, J. G. A. 1979, *Astron. Astrophys. Suppl.*, **35**, 1.

Emerson, J. P., and Jennings, R. E. 1978, *Astron. Astrophys.*, **69**, 129.

Fazio, G. G. 1978, in *Infrared Astronomy*, ed. G. Setti and G. G. Fazio (Reidel, Dordrecht), p. 25.

Fürst, E., Reich, W., and Sofue, Y. 1987, *Astron. Astrophys. Suppl.*, in press.

Gardner, F. F., and Whiteoak, J. B. 1975, *Monthly Notices Roy. Astron. Soc.*, **171**, 29P.

Gautier, T. N., Hauser, M. G., Beichman, C. A., Low, F. J., Neugebauer, G., Rowan-Robinson, M., Aumann, H. H., Boggess, N., Emerson, J. P., Harris, S., Houck, J. R., Jennings, R. E., and Marsden, P. L. 1984, *Astrophys. J. Letters*, **278**, L57.

Handa, T. 1987, Ph. D. Thesis, University of Tokyo.

Handa, T., Sofue, Y., Nakai, N., Hirabayashi, H., and Inoue, M. 1987, *Publ. Astron. Soc. Japan*, **39**, No. 5, in press.
Helfand, D. J., and Becker, R. H. 1987, *Astrophys. J.*, **314**, 203.
Kassim, N. E., LaRosa, T. N., and Erickson, W. C. 1986, *Nature*, **322**, 522.
Liszt, H. S. 1985, *Astrophys. J. Letters*, **293**, L65.
Lo, K. Y. 1986, *Science*, **233**, 1394.
Maihara, T., Oda, N., and Okuda, H. 1979, *Astrophys. J. Letters*, **227**, L129.
Mezger, P. G., and Pauls, T. 1979, in *The Large-Scale Characteristics of the Galaxy*, *IAU. Symp. No. 84*, ed. W. B. Burton (Reidel, Dordrecht), p. 357.
Morris, M., and Yusef-Zadeh, F. 1985, *Astron. J.*, **90**, 2511.
Reich, W., and Fürst, E. 1984, *Astron. Astrophys. Suppl.*, **57**, 165.
Reich, W., Fürst, E., Steffen, P., Reif, K., and Haslam, C. G. T. 1984, *Astron. Astrophys. Suppl.*, **58**, 197.
Reich, W., Sofue, Y., Wielebinski, R., and Seiradakis, J. H. 1987, *Astron. Astrophys.*, in press.
Seiradakis, J. H., Lasenby, A. N., Yusef-Zadeh, F., Wielebinski, R., and Klein, U. 1985, *Nature*, **317**, 697.
Sofue, Y. 1984, *Publ. Astron. Soc. Japan*, **36**, 539.
Sofue, Y. 1985, *Publ. Astron. Soc. Japan*, **37**, 697.
Sofue, Y., and Fujimoto, M. 1987, *Astrophys. J. Letters*, **319**, L73.
Sofue, Y., and Handa, T. 1984, *Nature*, **310**, 568.
Sofue, Y., and Reich, W. 1979, *Astron. Astrophys. Suppl.*, **38**, 251.
Sofue, Y., Reich, W., Inoue, M., and Seiradakis, J. H. 1987, *Publ. Astron. Soc. Japan*, **39**, 95.
Tsuboi, M., Inoue, M., Handa, T., Tabara, H., Kato, T., Sofue, Y., and Kaifu, N. 1986, *Astron. J.*, **92**, 818.
Uchida, Y., Shibata, K., and Sofue, Y. 1985, *Nature*, **317**, 699.
Yusef-Zadeh, F. 1986, Ph. D. Thesis, Columbia University, New York.
Yusef-Zadeh, F., Morris, M., and Chance, D. 1984, *Nature*, **310**, 557.
Yusef-Zadeh, F., Morris, M., Slee, O. B., and Nelson, G. J. 1986, *Astrophys. J. Letters*, **300**, L47.